Solid-phase interaction in ZrO_2–Fe_2O_3 nanocrystalline system

S. A. Kirillova[1], O. V. Almjasheva[1], V. V. Panchuk[2], V. G. Semenov[2]

[1]St. Petersburg State Electrotechnical University "LETI", ul. Professora Popova, 5, St. Petersburg, 197376, Russia
[2]St. Petersburg State University, Universitetskaya nab., 7–9, St. Petersburg, 199034, Russia

refractory-sveta@mail.ru, almjasheva@mail.ru, vitpan@mail.ru, val_sem@mail.ru

Based on the results of X-ray phase analysis and Mössbauer spectroscopy, it was demonstrated that in the ZrO_2–Fe_2O_3 system, represented by the mechanical mixture of m–ZrO_2 (14 ± 2 nm) and α-Fe_2O_3 (43 ± 2 nm) nanoparticles, being heated above the temperature corresponding to the melting temperature of the two-dimensional nonautonomous phase, transformation of α-Fe_2O_3 occurs resulting in appearing of the X-ray amorphous magnetically disordered state localized on the surface of ZrO_2 nanoparticles in the form of a thin layer. Transformation pattern in ZrO_2–Fe_2O_3 nanocrystalline system has been introduced.

Keywords: nanostructures, iron-zirconia, surface, X-ray diffraction, Mössbauer spectroscopy.

1. Introduction

Interest in systems containing zirconium dioxide is caused by high refractory properties, strength, crack resistance, chemical inertness, superionic oxygen conductivity, biocompatibility, catalytic activity and other important characteristics of the materials, based on this substance [1,2]. Ceramic and composite materials, based on ZrO_2–Fe_2O_3 system, are widely used as catalysts or catalyst carriers for hydrocarbons isomerization, carbon monoxide hydrogenization, selective hydrogenation (Fischer–Tropsch reaction) and ammonia synthesis [3,4], as well as the magnetic materials [5,6].

Different contradictory data, published in the scientific literature, are pertinent to possibilities and ranges of solid solutions formation in ZrO_2–Fe_2O_3 system. The study of phase formation processes in the considered system is connected with definite methodological difficulties, related to the behavior of the studied system components [7–16].

While extremely localized areas of the iron oxide-based solid solutions in zirconium dioxide may exist for the macroscopic particles, as it follows from data [17–26] (which is most pronounced for the low-temperature range), more wide solubility range of iron oxide in ZrO_2-based nanocrystals was detected, which is shown by data [27–36], in case of nano-scale particles. In this case, the possibility and the ranges of solid solutions existence in this system to a great degree are determined by the synthesis method of considered compositions.

Composition synthesis and subsequent study of their behavior during heating for ZrO_2–Fe_2O_3 system are generally realized with application of sol-gel synthesis followed by the annealing-quenching heat treatment of received precursors [16,22–24,31–33]; hydrothermal synthesis [5]; thermal decomposition of iron (III) and zirconium salts [27]; ZrO_2 impregnating with aqueous solution of ferric (III) nitrate and subsequent drying and incineration [3,4]; solid-phase synthesis method [25,37]; reaction media burning method (solid-phase flame method, solution burning) [26,38,39], etc. [6,34–36].

Inconsistencies pertinent to ranges of solid solutions areas, a state of ZrO_2 surface and iron ions location in different positions still exist and may be found almost in any new paper devoted to this system. Therefore, it is of interest to study the behavior of ZrO_2 and Fe_2O_3 nano-scale particles during their thermal treatment.

2. Experimental procedures

In order to study the solid-phase interaction of the components, ZrO_2 and Fe_2O_3 nano-scale powders, which have been obtained by hydrothermal treatment method (refer to [40]), were mixed in ethyl alcohol. Specimens were formed by pressing under pressure of 5 MPa, after which these specimens were heat treated in the air following the annealing-quenching mode with exposure during 30 minutes at temperatures of 800, 900, 1000 and 1100 °C.

The phase composition of the specimens was studied by X-ray phase analysis using XRD-7000 Shimadzu diffractometer (CuK_α-radiation). The X-ray diffraction pattern peak identification was performed using the PDWin 4.0 software solution and Crystallographica Search-Match package. Based on the data analysis pertinent to X-ray

diffraction pattern peak tailing, the average crystalline particle size has been calculated. Calculation was performed using the Sherrer equation [41].

The specimens' elemental composition was determined by electron probe microanalysis using Hitachi S-570 scanning electron microscope, equipped with Bruker Quantax 200 microprobe system.

Exposure of Mössbauer spectra was realized using WISSEL spectrometer operating in the constant acceleration mode, at the room temperature and at the liquid nitrogen boiling point. ^{57}Co in Rh-matrix, characterized by the radioactivity of 30 mC, was used as the source. Mathematical treatment of the experimental spectra was performed using the MOSSFIT software package [42]. The spectrometer velocity scale was calibrated using α-Fe foil at the room temperature. The chemical shift values were presented relative α-Fe.

3. Results and their discussion

Results of X-ray phase analysis of specimens, containing 6.4 ± 0.3 and 9.0 ± 0.6 mol.% $FeO_{1.5}$, which have been annealed at a temperature of 800, 900, 1000 and 1100 °C over 30 minutes, are presented in Figs. 1(*a*) and 2(*a*). Initial specimens were represented by the mechanical mixture of preliminary received nano-scale powders of ZrO_2 (monoclinic and tetragonal modification groups) and Fe_2O_3 [hematite, (104) peak, I – 100 %]. After heating at a temperature of 800 – 900 °C, a decrease in the intensity of the t-ZrO_2 peaks was observed, and after heating at a temperature above 900 °C, diffractograms contained only those reflections, which corresponded to monoclinic modification group of ZrO_2. For the specimen containing 6.4 ± 0.3 mol.% $FeO_{1.5}$, which was annealed at 800 and 900 °C, a peak on diffractograms, corresponding to α-Fe_2O_3, disappeared. During further increase of the thermal treatment temperature, (104) peak on diffractograms appeared again, however, its intensity was substantially less as compared with the initial composition. For the specimen, containing 9.0 ± 0.6 mol.% $FeO_{1.5}$, which has been annealed at a temperature of 800 – 900 °C, the relative intensity of (104) peak on diffractograms decreased as compared with the initial composition, while at a temperature of 1000 – 1100 °C the integral intensity of this peak has increased, becoming comparable with the initial composition.

It should be noted that sizes of m-ZrO_2 crystallites during heating up to a temperature of 900 °C have changed only slightly both for the specimen, containing 6.4 ± 0.3 mol.% $FeO_{1.5}$ (Fig. 3), as well as for the specimen, containing 9.0 ± 0.6 mol.% $FeO_{1.5}$. Analysis of m-ZrO_2 unit cell parameters dependence on temperature has demonstrated their invariability within the measurement accuracy (Fig. 4). Absence of variation of ZrO_2 unit cell parameters may be indicative of the fact that heat treatment during 30 minutes at a temperature of up to 1000 and 1100 °C did result in m-ZrO_2-based solid solution formation.

Mössbauer spectra for initial compositions of specimens, containing 6.4 ± 0.3 and 9.0 ± 0.6 mol.% $FeO_{1.5}$, as well as for specimens, annealed at 800, 900, 1000 and 1100 °C, are presented in Figs. 1(b) and 2(b), respectively. The results of experimental spectra analysis with detection of sextet and doublet components, corresponding to iron atoms in magnetically ordered and magnetically disordered phases, are also presented in Figs. 1(b) and 2(b). Mössbauer parameters for sextet and doublet components of the iron-containing phases are presented in Table 1. The quantitative estimation of the iron relative content in different phases was performed with precision determined by difference in values of f_M Mössbauer factor (probability of resonance absorption in each phase).

For the initial specimens, which were represented by the mechanical mixture of the preliminary produced t-, m-ZrO_2 and α-Fe_2O_3 nano-scale powders, the Mössbauer spectrum was characterized by sextet, parameters of which have corresponded to the sextet parameters for α-Fe_2O_3 [43].

For the specimens being thermally treated at 800 °C, the Mössbauer spectrum was characterized by doublet (6.4 ± 0.3 mol.% $FeO_{1.5}$) or doublet and sextet superposition (9.0 ± 0.6 mol.% $FeO_{1.5}$). It should be noted that for the specimen containing 6.4 mol.% $FeO_{1.5}$ only doublet components have been commonly observed, while these doublet components are incidental to the atoms of iron in 3+ oxidation rate located in the form of thin layer on the surface of another oxide [44, 45]. With a temperature increase, the sextet appeared again and the doublet share in experimental spectrum has decreased; at a temperature of 1100 °C a share of the magnetically disordered phase was about 23 %. Such an effect was observed in case of increasing of particles sizes [43]. For the specimen, containing 9.0 mol.% $FeO_{1.5}$, the sextet component is common for the whole heat treatment temperature range.

While comparing the data of X-ray phase analysis and Mssbauer spectroscopy, it may be concluded, that at a temperature of 800 °C, transformation of α-Fe_2O_3 begins, which results in its transfer into X-ray amorphous magnetically disordered phase, localized on the surface of zirconium dioxide particles, as shown by the absence of (104) α-Fe_2O_3 peak on the diffractogram, by sextet disappearance and doublet appearance in Mössbauer spectrum of the specimen, containing 6.4 ± 0.3 mol.% $FeO_{1.5}$. With increased thermal treatment temperatures, the sizes of m-ZrO_2 particles are increased (Fig. 3) that causes decrease of their surface area and, therefore, aggregation of the iron oxide surface layer, accompanied with α-Fe_2O_3 bulk phase particles formation. Formation of α-Fe_2O_3 particles is confirmed by the data of X-ray phase analysis and Mössbauer spectroscopy, i.e. (104) α-Fe_2O_3 peak
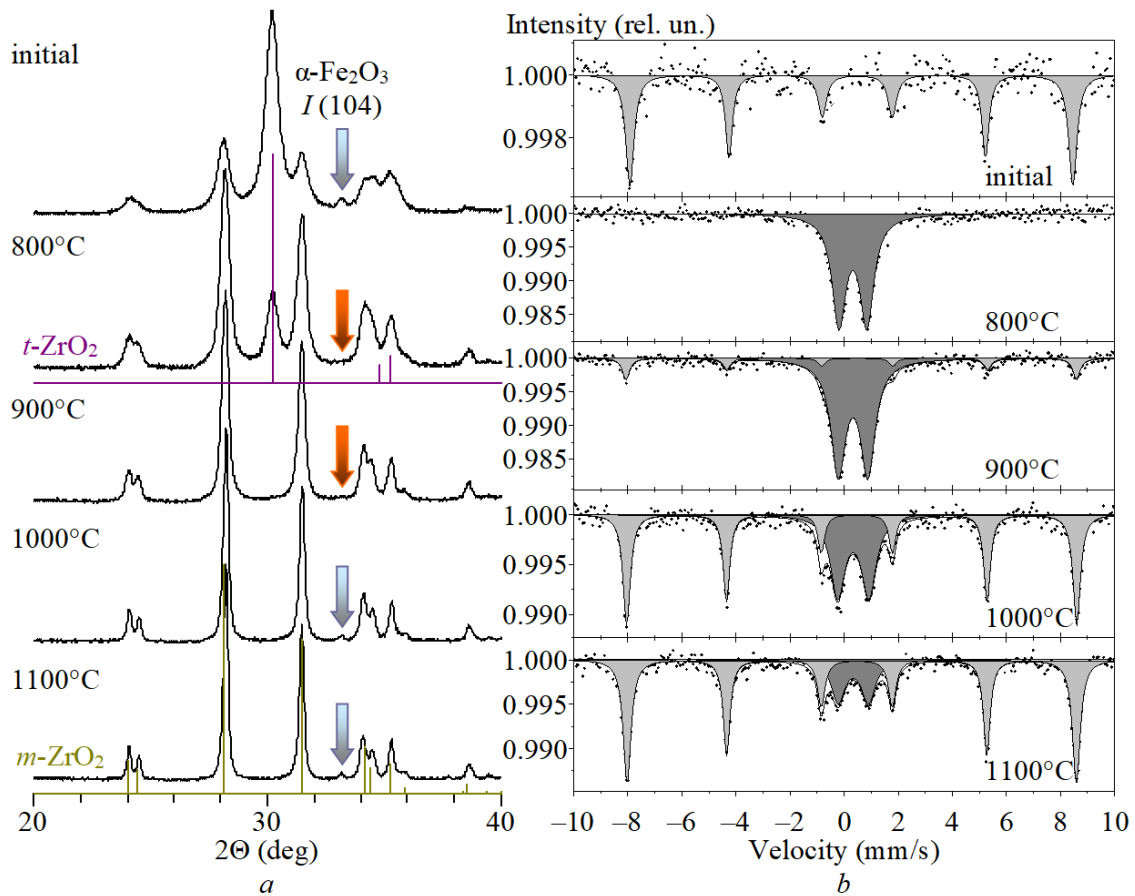
FIG. 1. X-ray diffractograms (*a*) and Mössbauer spectra series, measured at 25 °C (*b*) of the specimen, containing 6.4 ± 0.3 mol.% FeO$_{1.5}$, which has been annealed at a temperature of 800, 900, 1000 and 1100 °C during 30 minutes

on the diffractogram appears again, in Mössbauer spectrum for the specimen, containing 6.4 ± 0.3 mol.% FeO$_{1.5}$ sextet corresponding to α-Fe$_2$O$_3$, may be revealed against the doublet background.

Apparently, during thermal treatment at a temperature of 800 and 900 °C with exposure for 30 minutes, α-Fe$_2$O$_3$ is transformed with the formation of the iron oxide layer on a surface of ZrO$_2$ nanoparticles. At temperatures of 800 – 900 °C, for α-Fe$_2$O$_3$ are corresponding to the melting temperature of the surface (two-dimensional nonautonomous) phase [46]. It appears that transfer of the two-dimensional nonautonomous phase into a liquid (liquid-like) state initiates active mass transfer of the iron-containing component to a surface of ZrO$_2$ nanoparticles. It should be noted that similar processes were observed earlier in BeO–Fe$_2$O$_3$, MgO–Fe$_2$O$_3$, Al$_2$O$_3$–Fe$_2$O$_3$, SiO$_2$–Fe$_2$O$_3$ systems [44, 45]. The transformation pattern, corresponding to the described processes in ZrO$_2$–Fe$_2$O$_3$ system, in which zirconium dioxide is initially represented by m-ZrO$_2$ and by α-Fe$_2$O$_3$ nanoparticles, characterized by the crystallites sizes of 14 ± 2 nm and 43 ± 2 nm, respectively, is presented in Fig. 5.

4. Conclusion

As distinct from the cases, in which compositions are received via codeposition, hydrothermal synthesis, etc., and in which mixing of components is initially possible at the atomic level, in the case of the solid-phase interaction of the nano-scale particles in ZrO$_2$–Fe$_2$O$_3$ system in the range of low contents of the iron-containing component increasing of the treatment temperature up to 800 – 900 °C does not cause stabilization of zirconium dioxide tetragonal modification and the formation of tetragonal solid solution, as well as Fe^{3+} ions are not included into m-ZrO$_2$ structure.

During the thermal treatment of ZrO$_2$ and Fe$_2$O$_3$ nanoparticles, at definite critical value of temperature in range of 800 – 900 °C, α-Fe$_2$O$_3$ transformation occurs with thin layer formation on m-ZrO$_2$ nanoparticles surface, i.e. formation of the composite nanoparticles of "nucleus (m-ZrO$_2$ nanoparticles) – shell (amorphous Fe$_2$O$_3$)" type takes place.
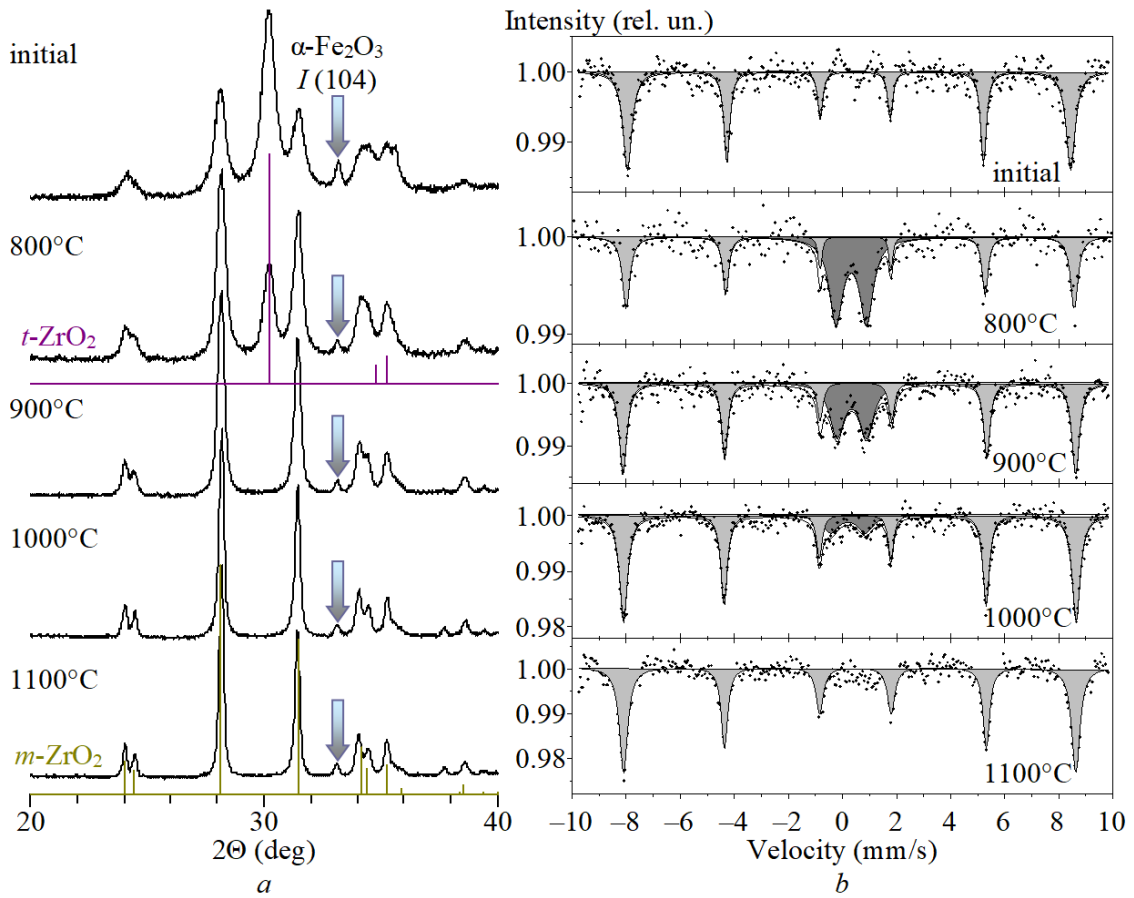
FIG. 2. X-ray diffractograms (*a*) and Mössbauer spectra series, measured at 25 °C (*b*) of the specimen, containing 9.0 ± 0.6 mol.% $FeO_{1.5}$, which has been annealed at a temperature of 800, 900, 1000 and 1100 °C during 30 minutes
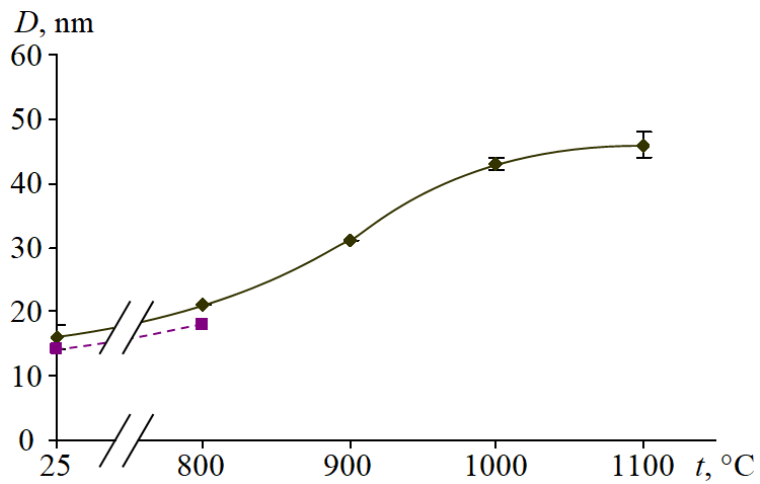

FIG. 3. t-ZrO_2 (■) and m-ZrO_2 (♦) crystallites sizes dependence on the heat treatment temperature for the specimen, containing 6.4 ± 0.3 mol.% $FeO_{1.5}$
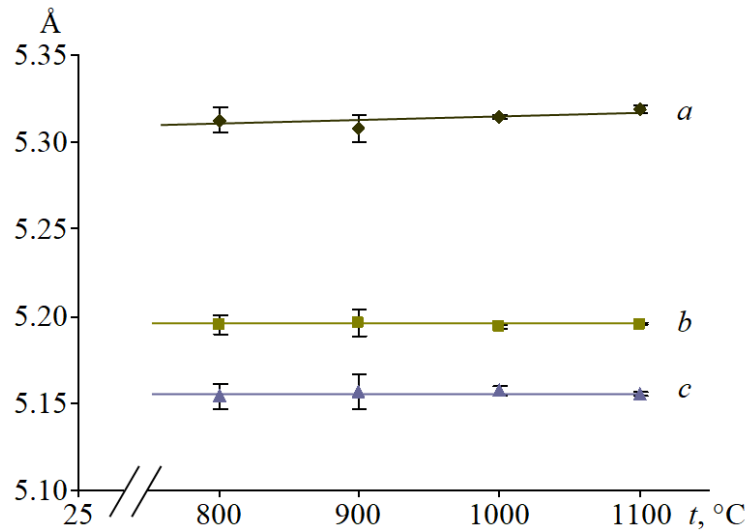
FIG. 4. m-ZrO$_2$ unit cell parameters dependence on the heat treatment temperature for the specimen, containing 6.4 ± 0.3 mol.% FeO$_{1.5}$

TABLE 1. Mössbauer parameters of spectra, measured for the studied specimens at a temperature of 25 °C

FeO$_{1.5}$ content, mol.%	Annealing temperature, °C	Parameters of Mössbauer spectra					
		sextet			doublet		Paramagnetic component content, %
		Isomer shift, mm/s	Quadrupole splitting, mm/s	Effective field, T	Isomer shift, mm/s	Quadrupole splitting, mm/s	
6.4±0.3	–	0.378±0.013	0.218±0.026	50.871±0.099	–	–	0
	800	–	–	–	0.326±0.000	1.032±0.000	100
	900	0.375±0.018	0.221±0.037	51.734±0.122	0.331±0.000	1.092±0.011	84.85
	1000	0.376±0.005	0.188±0.010	51.693±0.038	0.340±0.014	1.152±0.029	41.51
	1100	0.376±0.004	0.185±0.007	51.594±0.028	0.337±0.021	1.123±0.042	22.62
9.0±0.6	–	0.357±0.005	0.228±0.010	50.905±0.040	–	–	0
	800	0.383±0.016	0.192±0.033	51.458±0.136	0.324±0.042	1.128±0.080	52.54
	900	0.374±0.008	0.240±0.015	51.984±0.060	0.342±0.040	1.093±0.078	35.01
	1000	0.372±0.005	0.193±0.009	51.976±0.037	0.203±0.077	1.292±0.169	14.18
	1100	0.373±0.006	0.211±0.011	51.938±0.044	0.193±0.087	1.282±0.179	~ 5
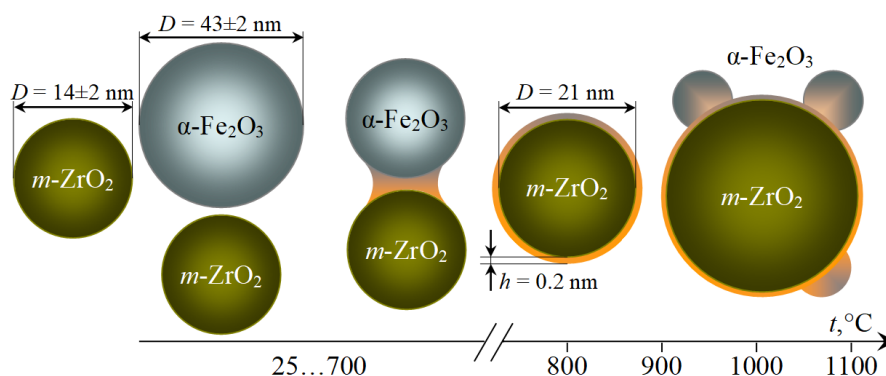
Fig. 5. Transformation pattern in ZrO_2–Fe_2O_3 system

References

[1] Shackelford J.F., Doremus R.H. *Ceramic and Glass Materials. Structure, Properties and Processing*. Springer, Boston, MA, 2008, 209 p.

[2] Almjasheva O.V., Garabadzhiu A.V., Kozina Yu.V., et al. Biological effect of zirconium dioxide-based nanoparticles. *Nanosystems: Phys. Chem. Math.*, 2017, **8** (3), P. 391–396.

[3] Chen K., Dong L., Yan Q., Chen Y. Dispersion of Fe_2O_3 supported on metal oxides studied by Mssbauer spectroscopy and XRD. *J. Chem. Soc., Faraday Trans.*, 1997, **93** (12), P. 2203–2206.

[4] Okamoto Y., Kubota T., Ohto Y., Nasu S. Metal Oxide–Support Interactions in Fe/ZrO_2 Catalysts. *J. Phys. Chem. B*, 2000, **104** (35), P. 8462–8470.

[5] Kuryliszyn-Kudelska I., Arciszewska M., Maolepszy A., et al. Influence of Fe doping on magnetic properties of ZrO_2 nanocrystals. *J. Alloys Compd.*, 2015, **632**, P. 609–616.

[6] de Souza A.O., Ivashita F.F., Biondo V., et al. Structural and magnetic properties of iron doped ZrO_2. *J. Alloys Compd.*, 2016, **680**, P. 701–710.

[7] Belov G.V., Iorish V.S., Yungman V.S. IVTANTHERMO for Windows – database on thermodynamic properties and related software. *Calphad: Comput. Coupling Phase Diagrams Thermochem.*, 1999, **23** (2), P. 173–180.

[8] Srinivasan R., Davis B.H., Burl C.O., Hubbard C.R. Crystallization and phase transformation process in zirconia: an in situ high-temperature X-ray diffraction study. *J. Am. Ceram. Soc.*, 1992, **75** (5), P. 1217–1222.

[9] Oleinikov N.N., Pentin I.V., Murav'eva G.P., Ketsko V.A. Highly disperse metastable ZrO_2-based phases. *Russ. J. Inorg. Chem.*, 2001, **46** (9), P. 1275–1281.

[10] Guo X., Schober T. Water incorporation in tetragonal zirconia. *J. Am. Ceram. Soc.*, 2004, **87** (4), P. 746–748.

[11] Shukla S., Seal S. Mechanisms of room temperature metastable tetragonal phase stabilisation in zirconia. *Int. Mater. Rev.*, 2005, **50** (1), P. 45–64.

[12] Zhang F., Chupas P.J., Lui S.L.A., et al. In situ study of the crystallization from amorphous to cubic zirconium oxide: Rietveld and reverse Monte Carlo analyses. *Chem. Mater.*, 2007, **19** (13), P. 3118–3126.

[13] Lin F.-Q., Dong W.-S., Liu C.-L., et al. In situ source–template-interface reaction route to hollow ZrO_2 microspheres with mesoporous shells. *J. Colloid Interface Sci.*, 2008, **323** (2), P. 365–371.

[14] Almjasheva O.V. Heat-stimulated transformation of zirconium dioxide nanocrystals produced under hydrothermal conditions. *Nanosystems: Phys. Chem. Math.*, 2015, **6** (5), P. 697–703.

[15] Li F., Li Y., Song Z., et al. Evolution of the crystalline structure of zirconia nanoparticles during their hydrothermal synthesis and calcination: Insights into the incorporations of hydroxyls into the lattice. *J. Eur. Ceram. Soc.*, 2015, **35** (8), P. 2361–2367.

[16] Li P., Chen I-W., Penner-Hahn J.E. Effect of dopants on zirconia stabilization – An X-ray Absorption Study: I, Trivalent Dopants. *J. Am. Ceram. Soc.*, 1994, **77** (1), P. 118–128.

[17] Muan A. Phase equilibria at high temperatures in oxide systems involving changes in oxidation states. *Am. Jour. Sci.*, 1958, **256** (3), P. 171–207.

[18] Jones T., Kimura S., Muan A. Phase Relations in the System FeO–Fe_2O_3–ZrO_2–SiO_2. *J. Am. Ceram. Soc.*, 1967, **50** (3), P. 137–142.

[19] Petrov Yu.B., Udalov Yu.P., Slovak J., Morozov Yu.G. Liquid immiscibility phenomena in melts of the ZrO_2–FeO–Fe_2O_3 System. *Glass Phys. Chem.*, 2002, **28** (3), P. 139–146.

[20] Bechta S.V., Krushinov E.V., Al'myashev V.I., et al. Phase relations in the ZrO_2–FeO system. *Russ. J. Inorg. Chem.*, 2006, **51** (2), P. 325–331.

[21] Bechta S.V., Krushinov E.V., Almjashev V.I., et al. Phase diagram of the ZrO_2–FeO system. *J. Nucl. Mater.*, 2006, **348** (1–2), P. 114–121.

[22] Popović S., Gržeta B., Czakó-Nagy I., Musić S. Structural properties of the system m-ZrO_2–α-Fe_2O_3. *J. Alloys Compd.*, 1996, **241** (1–2), P. 10–15.

[23] Kriventsov V.V., Kochubey D.I., Maximov Yu.V., et al. Structural determination of the Fe-modified zirconium oxide. *Nucl. Instrum. Methods Phys. Res., Sect. A*, 2001, **470** (1–2), P. 341–346.

[24] Navo J.A., Hidalgo M.C., Coln G., et al. Preparation and Physicochemical Properties of ZrO_2 and Fe/ZrO_2 Prepared by a Sol-Gel Technique. *Langmuir*, 2001, **17** (1), P. 202–210.

[25] Beck H.P., Kaliba C. On the solubility of Fe, Cr and Nb in ZrO_2 and its effect on thermal dilatation and polymorphic transition. *Mater. Res. Bull.*, 1990, **25** (9), P. 1161–1168.

[26] Ghigna P., Spinolo G., Anselmi-Tamburini U., et al. Fe-Doped Zirconium Oxide Produced by Self-Sustained High-Temperature Synthesis: Evidence for an Fe–Zr Direct Bond. *J. Am. Chem. Soc.*, 1999, **121** (2). P. 301–307.

[27] Davison S., Kershaw R., Dwight K., Wold A. Preparation and characterization of cubic ZrO₂ stabilized by Fe(III) and Fe(II). *J. Solid State Chem.*, 1988, **73** (1), P. 47–51.

[28] Inwang I.B., Chyad F., McColm I.J. Crystallisation of iron(III)-zirconia co-gels. *J. Mater. Chem.*, 1995, **5** (8), P. 1209–1213.

[29] Berry F.J., Loretto M.H., Smith M.R. Iron-zirconium oxides: An investigation of structural transformations by X-ray diffraction, electron diffraction, and iron-57 Mössbauer spectroscopy. *J. Solid State Chem.*, 1989, **83** (1), P. 91–99.

[30] Berry F.J., Jobsen S., Smith M.R. Iron-zirconium oxide catalysts for the hydrogenation of carbon monoxide: In situ studies by iron-57 Mössbauer spectroscopy. *Hyperfine Interact.*, 1989, **46** (1), P. 607–611.

[31] Štefanić G., Musić S., Popović S., Nomura K. A study of the ZrO₂–Fe₂O₃ system by XRD, ^{57}Fe Mössbauer and vibrational spectroscopies. *J. Mol. Struct.*, 1999, **480–481**, P. 627–631.

[32] Štefanić G., Gržeta B., Musić S. Influence of oxygen on the thermal behavior of the ZrO₂–Fe₂O₃ system. *Mater. Chem. Phys.*, 2000, **65** (2), P. 216–221.

[33] Štefanić G., Gržeta B., Nomura K., et al. The influence of thermal treatment on phase development in ZrO₂–Fe₂O₃ and HfO₂–Fe₂O₃ systems. *J. Alloys Compd.*, 2001, **327** (1–2), P. 151–160.

[34] Jiang J.Z., Poulsen F.W., Mrup S. Structure and thermal stability of nanostructured iron-doped zirconia prepared by high-energy ball milling. *J. Mater. Res.*, 1999, **14** (4), P. 1343–1352.

[35] Cao W., Tan O.K., Zhu W., et al. An amorphous-like $x\alpha$-Fe₂O₃–$(1-x)$ZrO₂ solid solution system for low temperature resistive-type oxygen sensing. *Sens. Actuators, B*, 2001, **77** (1–2), P. 421–426.

[36] Kiminami R.H.G. The monoclinic-tetragonal phase transformation of zirconia in the system ZrO₂–Fe₂O₃. *J. Mater. Sci. Lett.*, 1990, **9** (4), P. 373–374.

[37] Bohé A.E., Andrade Gamboa J.J., Pasquevich D.M. Enhancement of the martensitic transformation of tetragonal zirconia powder in the presence of iron oxide. *Mater. Sci. Eng., A*, 1999, **273–275**, P. 218–221.

[38] Maglia F., Anselmi-Tamburini U., Spinolo G., Munir Z.A. Thermal Stability of Combustion-Synthesized Metastable Solid Solutions of Zirconia and Transition Metals. *J. Mater. Synth. Process.*, 1999, **7** (5), P. 327–332.

[39] Garcia F.L., de Resende V.G., De Grave E., et al. Iron-stabilized nanocrystalline ZrO₂ solid solutions: Synthesis by combustion and thermal stability. *Mater. Res. Bull.*, 2009, **44** (6), P. 1301–1311.

[40] Pozhidaeva O.V., Korytkova E.N., Drozdova I.A., Gusarov V.V. Phase state and particle size of ultradispersed zirconium dioxide as influenced by conditions of hydrothermal synthesis. *Russ. J. Gen. Chem.*, 1999, **69** (8), P. 1219–1222.

[41] Patterson A.L. The Scherrer formula for x-ray particle size determination. *Phys. Rev.*, 1939, **56** (10), P. 978–982.

[42] Semenov V.G., Moskvin L.N., Efimov A.A. Analytical potential of Mössbauer spectroscopy. *Russ. Chem. Rev.*, 2006, **75** (4), P. 317–327.

[43] Suzdalev I.P. *Electrical and magnetic transitions in nanoclusters and nanostructures*. KRASAND, Moscow, 2012, 480 p. (in Russian)

[44] Gusarov V.V., Egorov F.K., Ekimov S.P., Suvorov S.A. Mössbauer study of the kinetics of the formation of film states in the interaction of oxides of magnesium and iron. *J. Phys. Chem.*, 1987, **61** (6), P. 1652–1654. (in Russian)

[45] Gusarov V.V., Malkov A.A., Malygin A.A., Suvorov S.A. Thermally activated transformations of 2D nonautonomous phases and contradiction of polycrystalline oxide materials. *Inorg. Mater.*, 1995, **31** (3), P. 320–323.

[46] Gusarov V.V., Suvorov S.A. Melting points of locally equilibrium surface phases in polycrystalline systems based on a single volume phase. *J. Appl. Chem. of the USSR*, 1990, **63** (8), P. 1560–1565.